

Nanocrystalline aluminium hydrides for hydrogen storage

Maximilian Fichtner*, Jens Engel, Olaf Fuhr, Oliver Kircher, Oliver Rubner

Institute for Nanotechnology, Research Centre Karlsruhe GmbH, POB 3640, D-76021 Karlsruhe, Germany

Abstract

Nanocrystalline aluminium hydrides (alanates) are potential hydrogen storage materials for PEM fuel cell applications. Beside the reversible amount of hydrogen, kinetic and thermodynamic properties of alanate-based storage materials have still to be optimised. Progress was made in improving the kinetics of hydrogen uptake and release by a novel Ti catalyst. The available base materials, however, suffer from the low hydrogen content or unfavourable thermodynamic properties. Magnesium alanate has the potential to exchange up to 6.9 wt.% of hydrogen in its first transformation step. First measurements indicate equilibrium desorption pressures above 100 bar at the working temperatures of a PEM fuel cell.

© 2003 Elsevier B.V. All rights reserved.

Keywords: Hydrogen storage; Metal hydrides; Alanates

1. Introduction

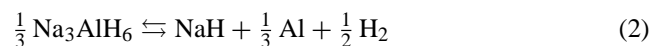
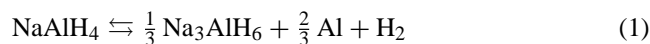
Several challenges have to be met in the development of novel materials for hydrogen storage. A key issue is the reversible content of hydrogen which can be obtained in cycle tests. Secondly, the kinetics of hydrogen absorption and desorption are important, especially if the development aims at an application in fuel cell driven automobiles. Moreover, the thermodynamic properties of the material will determine pressure and temperature ranges where the storage material can be operated and they set the requirements for a heat management system.

One of the 2010 technical targets of the US-DOE for on-board hydrogen storage is to overcome a “commercialisation barrier” of about 6 wt.% hydrogen a storage material should contain [1]. At the same time the density of the material should not be too low so that the volume of the tank stays in an acceptable range. The DOE target for the refuelling time was set to <5 min. The upper operating temperature of the storage is defined and limited by the working temperature of the PEM fuel cell (currently 80–100 °C).

There is no compound amongst the classical low temperature metal hydrides which would fit to these recommendations as the storage capacity of the known systems is limited to about 2 wt.% which was found with a Laves phase material [2].

The complex metal hydrides ($M^{n+}[NH_m]_n^-$, with M, N = metal) offer higher hydrogen storage capabilities instead. Amongst them, the aluminium hydrides (alanates, N = Al, $m = 4$) and boranates (N = B, $m = 4$) have the highest storage capacities of the solid metal hydrides, up to 18 wt.% ($LiBH_4$). But up to now there has been only one compound identified which shows experimentally proven reversibility in terms of hydrogen uptake and release under moderate conditions, the sodium aluminium hydride, or sodium alanate ($NaAlH_4$).

From its content of 7.5 wt.% H, 5.6 wt.% should theoretically be available from the reversible decomposition reactions, Eqs. (1) and (2). The third step, the decomposition of NaH, Eq. (3), occurs at temperatures above 400 °C which is considered too high for most technical applications [3].



When Ti dopants are added to the pure sodium alanate [4], interfering kinetic barriers can be lowered and the transformations in steps (1) and (2) can be accomplished at temperatures around 100 °C. However, the dissociation pressure of the second step, Eq. (2), crosses the 1 bar line at around 110 °C in the Van't Hoff plot. Hence, a decomposition against vacuum would be necessary to achieve a hydrogen release which is fast enough in that temperature range.

* Corresponding author.

E-mail address: fichtner@int.fzk.de (M. Fichtner).

With catalytically doped sodium alanate, a technically reversible content of about 4.5 wt.% was found by most of the working groups [5–7]. The difference of about 1 wt.% between the theoretical value and the amount determined in cycle tests has been explained by an incomplete back-reaction of Na_3AlH_6 , Al and H_2 into NaAlH_4 (Eq. (1)) [6,8].

Ball milling of the pure compound or mixed lithium and sodium aluminium hydrides leads to beneficial effects [8] as the kinetics for the hydrogen exchange can be increased and, in case of the mechanically synthesised mixed alanates, the equilibrium pressure for a given temperature can be lowered.

For technical applications, the kinetics of hydrogen uptake and release is an important issue. The absorption kinetics of NaAlH_4 have been regarded as a particular problem, because the process is slow and only 10% rehydrogenation can be achieved within 15 h at 170 °C and 152 bar [4]. Various authors reported that Ti-based compounds are the most effective dopants, while the best results were obtained with solid Ti halides, which were ball-milled together with the alanate. In this paper, we report that a considerable improvement is possible when small Ti clusters are used for the catalysis of hydrogen exchange.

Other alanates with higher hydrogen contents have either unfavourable properties, are not available as in the case of $\text{Ti}(\text{AlH}_4)_4$ and $\text{Zr}(\text{AlH}_4)_4$ or have not been investigated sufficiently. LiAlH_4 contains 10.6 wt.% of H, and a theoretical amount of 7.9 wt.% would be usable for hydrogen storage if the reaction steps according to Eqs. (1) and (2) were reversible. Unfortunately, the compound exhibits unfavourable thermodynamic properties. The reaction enthalpy of the first step is negative at room temperature, which means that the material is unstable and cannot be reloaded with hydrogen [8].

Besides the light weighted alkali alanates, the earth alkaline compound $\text{Be}(\text{AlH}_4)_2$ with 11.3 wt.% of H contains the toxic and carcinogenic beryllium. Magnesium alanate, $\text{Mg}(\text{AlH}_4)_2$, is currently the only stable alanate which contains enough hydrogen to overcome the commercialisation barrier and which has a sustainable elemental composition. Magnesium alanate is a complex aluminium hydride which contains a theoretical amount of 9.3 wt.% of hydrogen. After the first report of the synthesis of the compound [9] in 1950, it has hardly been investigated and little is known about the material and its suitability for reversible hydrogen storage. In the following, results are presented on the structure and thermal properties of magnesium alanate.

2. Experimental

All sample preparations were done in an argon-filled glove box equipped with a recirculation system to keep the water and oxygen concentrations below 1 ppm during operation. Properties and treatment of the chemicals used for the syntheses and for doping are described elsewhere [7,9].

High energy ball milling has been performed with a FRITSCH P6 with 600 rpm using a 80 ml silicon nitride vial and balls (ball-to-powder ratio 20:1). Milling was done under an argon atmosphere.

Volumetric measurements were performed with a modified Sieverts apparatus. Hydrogen pressures of up to 200 bar can be applied and the values are monitored using piezoresistive high precision pressure transducers. A description of the apparatus is given in [7].

Thermogravimetric analysis was conducted under vacuum between room temperature and 400 °C at a heating rate of 2 K/min using a NETZSCH STA 409C analyser equipped with a BALZERS quadrupole mass spectrometer for analysis of the evolved gas.

Raman measurements were carried out at room temperature with a WITec CRM 200 Raman microscope using a 600 grooves/mm grating, focused at 2400 cm^{-1} . In this setting spectra were taken in the range between 170 and 4100 cm^{-1} , with an uncertainty of about $\pm 7\text{ cm}^{-1}$. The instrument was calibrated with silicon. The wavelength of the incident light was 514.5 nm generated by an argon-ion laser with an effective power of 5.3 mW at the sample. Data acquisition was made in the given range by accumulating 10 spectra of 60 s. Nanocrystalline $\text{Mg}(\text{AlH}_4)_2$ was filled in a flat washer between a carrier glass and a thin cover glass, both sealed with silicon grease to inhibit contact with air and moisture.

The Raman spectra were further analysed by using line fitting procedures and Gaussian line shapes with the help of the ORIGIN 6.0 PFM program module.

3. Results

3.1. Catalysis of hydrogen exchange with NaAlH_4

Several attempts have been made to investigate the role and nature of the Ti catalyst. From the current state in the literature it is, nevertheless, an open question, whether the Ti is active in a finely dispersed form at the surface of the hydride or whether it substitutes atoms in the alanate lattice, or whether both states contribute to the catalytic effect. The role of the dispersion, which stands for the fraction of exposed active metal atoms of the catalyst, has not been determined yet.

In a first approach, we synthesised colloidal Ti following a procedure in the literature [11]. Two-shell Ti clusters were obtained as was determined by EXAFS measurements [7]. According to FTIR measurements, elemental analysis and X-ray absorption measurements the clusters consisted of 13 Ti atoms which are stabilised by six THF ligands ($\text{Ti}_{13}\cdot 6\text{THF}$). It has been suggested that one THF molecule is bound by three Ti atoms [11]. The proposed structure of the clusters is shown in the inset of Fig. 1.

Fig. 1 shows the desorption behaviour of three differently doped NaAlH_4 samples. Two mol% of TiCl_3 were added

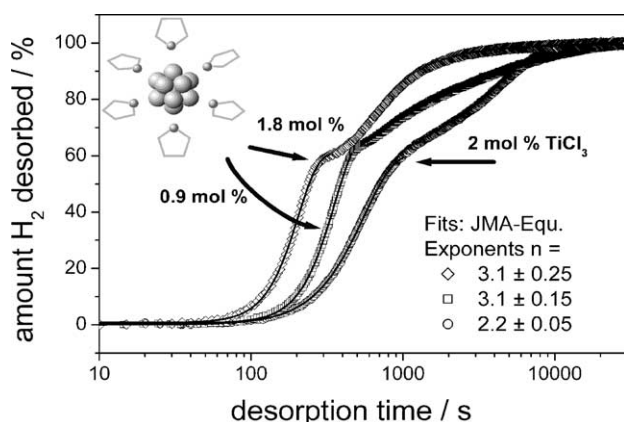


Fig. 1. Dehydrogenation of three differently catalysed samples at 150 °C. The curves are normalised to 100% desorption which was equivalent to 4.5 ± 0.1 wt.% H in all measurements.

in one experiment (right curve), 0.9 and 1.8 mol% Ti as Ti colloid were added in the two other experiments. In each case, the dopants were ball-milled together with the alanate for 30 min. The results clearly show the superior desorption kinetics for the cluster catalysed samples when compared to the standard catalyst. The stair-like increase reflects the two-step desorption behaviour which can be expected from Eqs. (1) and (2).

The shape of the curves is typical for the decomposition of solids controlled by nucleation and growth of new phases. Such a behaviour can also be found with the classical metal hydrides [12]. Regarding the first decomposition step, it is apparent that the shapes of the two cluster catalysed samples are similar and differ from the shape of the TiCl_3 catalysed sample. A fit according to the Johnson–Mehl–Avrami (JMA) theory to the first desorption step up to 60% desorption is shown in the diagram. Two different exponents were obtained for the cluster catalysed samples (3.1 ± 0.2) and for the TiCl_3 catalysed sample (2.2 ± 0.05). The difference may indicate different growth dimensionalities of the nuclei if the growth of the new phase is controlled by hydride-metal interface processes. In order to obtain experimental evidence of possible changes in the rate limiting step and/or in the growth dimensionality, further investigations are in process.

In Fig. 2 the absorption rate of hydrogen by a Ti cluster catalysed sample is compared to the state-of-the art in the literature: A sample which was prepared by adding 2 mol% of TiCl_3 to pure NaAlH_4 and ball-milling the mixture under argon atmosphere for 3 h. After decomposition it was reloaded to 80% of the maximum reversible capacity (4.5 wt.%) at 125 °C, 91 bar hydrogen, within about 35 min [5]. Compared with this, a sample which was prepared by ball-milling (Ar atmosphere, 30 min) pure NaAlH_4 , doped with 1.8 mol% Ti from Ti clusters was reloaded in the third cycle to 80% within only 7 min, at 100 °C and 100 bar hydrogen pressure. This time is close to the 2010 target for the refuelling of a hydrogen storage material.

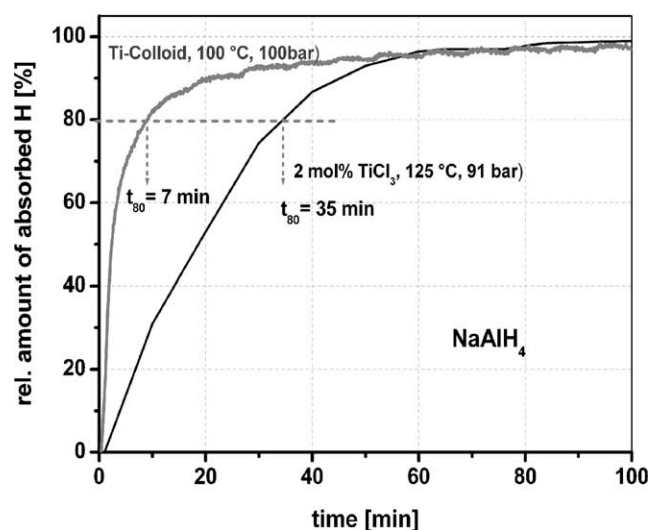
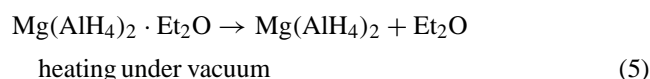
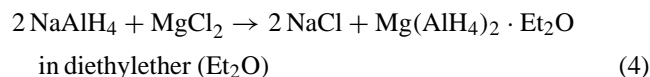


Fig. 2. Hydrogen absorption of a Ti cluster catalysed sample compared to the state-of-the art in the literature [5].

The theoretical amount of Ti in $\text{Ti}_{13}\cdot 6\text{THF}$ (59% Ti) is much higher compared to other compounds such as TiF_3 (45.7% Ti), TiCl_3 (31% Ti) or $\text{Ti}(\text{BuO})_4$ (14% Ti). The hydrogenation and dehydrogenation measurements indicate, however, that the state of the precursor is of even greater importance than the simple amount of Ti in the material. The experiments show rather that the size of the Ti particles is crucial for the activity of the catalyst.

3.2. Properties of $\text{Mg}(\text{AlH}_4)_2$

Pure $\text{Mg}(\text{AlH}_4)_2$ has been synthesised in gram amounts by a metathesis reaction of MgCl_2 and NaAlH_4 , in diethylether as solvent, Eq. (4), followed by a purification and a drying procedure, Eq. (5). The final product has been obtained with a purity of about 95% with impurities of NaCl and hydrocarbons. Experimental details are given elsewhere [10].



Single crystals from the diethylether adduct could be obtained in step (4). X-ray diffraction (XRD) measurements were performed with these crystals in order to determine the crystal structure of the ether adduct. This has, however, not been possible with the end product, because the crystalline material decomposes in step (5) and the obtained magnesium alanate has always been an ultrafine powder. Its mean crystallite size has been in the range of 30–40 nm, depending on the conditions of the drying procedure.

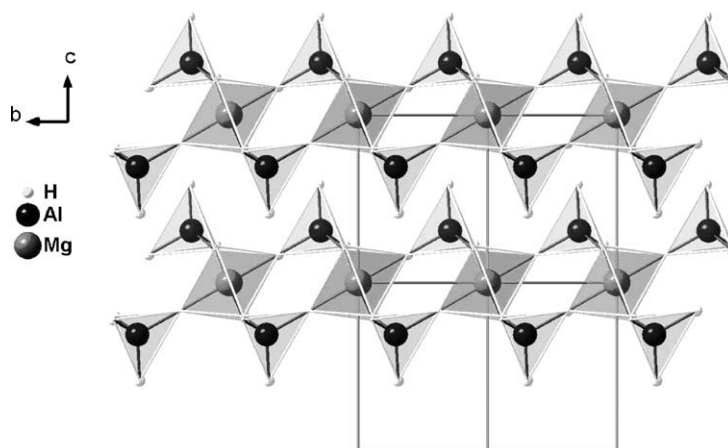


Fig. 3. Crystal structure of magnesium alanate. View from the a -axis, perpendicular to two alanate sheets. The grey lines represent the unit cell.

3.2.1. Structure

To determine the structure of $\text{Mg}(\text{AlH}_4)_2$, our first approach was to interpret FTIR and X-ray diffraction data of the solvent adducts and the FTIR data of the pure alanate, leading to a first guess for the structure [10]. Subsequently, electronic structure calculations were performed for MgAl_2H_8 clusters using density functional theory in order to develop a crystal structure. The calculated atomic positions were verified by comparison of a simulated XRD pattern with experimental XRD data [13].

According to these results, $\text{Mg}(\text{AlH}_4)_2$ exhibits a sheet structure, the sheets consisting of tilted MgH_6 octahedra which are interconnected by AlH_4 tetrahedra (Fig. 3). Three of the four H atoms of each tetrahedron serve as hydrogen

bridges, one H atom always has a terminal bond. The structure with the space group $P-3m1$ has a trigonal symmetry and resembles the structure of CdI_2 , with the Cd atoms replaced by Mg and the iodine atoms replaced by AlH_4 groups. It is the first reported sheet structure of an alanate.

Additional support for the trigonal symmetry (C_{3v}) at the AlH_4 tetrahedra comes from Raman data. The Raman spectrum of magnesium alanate (Fig. 4) shows six signals, as expected from the theory. Three of them can be attributed to two A and a doubly degenerated E vibration in the region of the stretching vibrations between 1800 and 2000 cm^{-1} . Another set of two A and a doubly degenerated E vibration can be found in the fingerprint region between 600 and 1000 cm^{-1} .

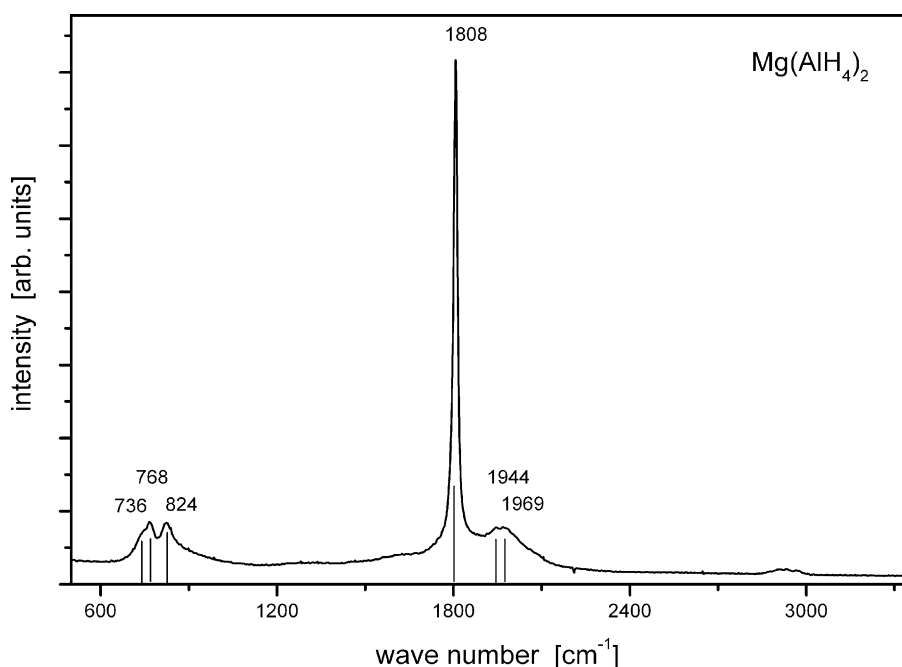


Fig. 4. Raman spectrum of $\text{Mg}(\text{AlH}_4)_2$ measured at room temperature. The vertical lines indicate the peak positions which were determined in the fitting procedure.

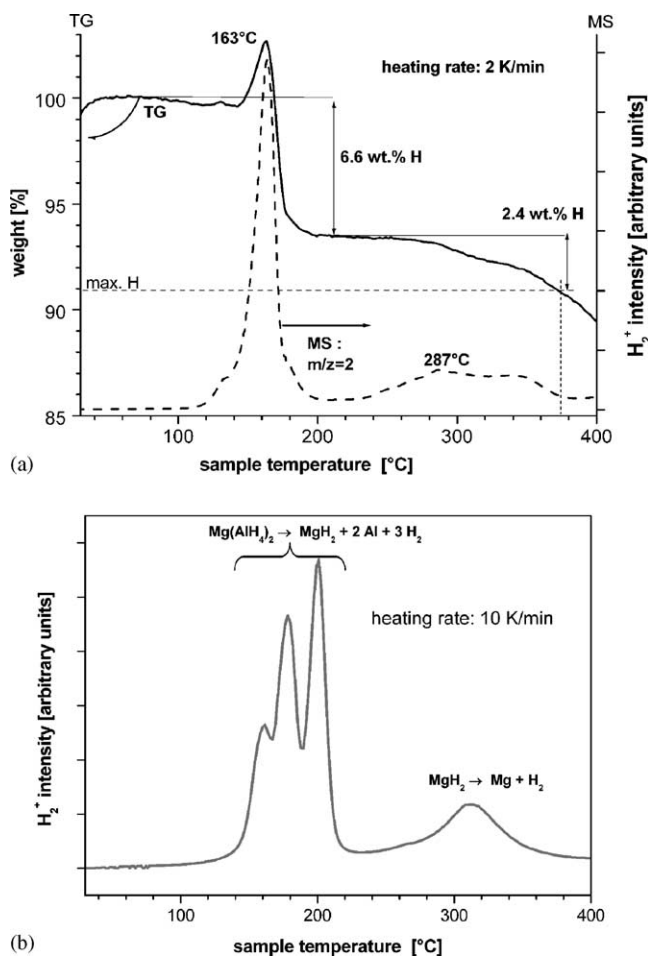
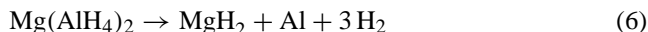


Fig. 5. TGA-MS data of the thermal decomposition of $\text{Mg}(\text{AlH}_4)_2$. (a) At a heating rate of 2 K/min. (b) MS signal at a heating rate of 10 K/min.

3.2.2. Thermal decomposition

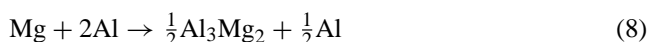
To investigate the thermal decomposition of the magnesium alanate, TGA-MS experiments have been performed. As can be seen from Fig. 5, the alanate decomposes in two major steps instead of the three which are known from the alkaline alanates (reactions (1)–(3)). In the first step, the $\text{Mg}(\text{AlH}_4)_2$ releases three quarters of the bound hydrogen, with a peak decomposition temperature of 163 °C, in vacuum. The solid product of the first decomposition step has been analysed by XRD and consists of a mixture of MgH_2 and Al. Hence, the following transition occurs:



At temperatures around 300 °C, the magnesium hydride decomposes and the magnesium reacts with the metallic Al to form an intermetallic compound, as was detected by XRD measurements [14]. The following transition occurs in the second step:



followed by the reaction:



These equations give only a rough idea of what is going on in the material when it gets decomposed. The plot of the MS intensity at $m/z = 2$ in Fig. 5a shows that there seems to be several contributions to the first signal, which may be due to different transformation steps. Temperature programmed XRD measurements in this temperature range did, however, not reveal any intermediate crystalline phases which may be due to several reasons: Either the stationary concentration of an intermediate crystalline phase is below the detection limit of the method which may occur when a relatively slow formation of the intermediate is followed by a relatively fast subsequent reaction. Another possibility is that the intermediate is not crystalline and has to be detected by other analytical methods.

An indication for the existence of several transformation steps during the transition in Eq. (6) is shown in Fig. 5b. There, the MS intensity of the molecular hydrogen is plotted for a heating rate of 10 K/min. The diagram shows that the signal shown in Fig. 5a is resolved into three contributions when the heating rate is increased. The difference in the thermal shift of the underlying transformations indicates that these steps have different activation energies. The relative intensities of the contributions may vary and seem to be influenced by impurities in the sample. Residual organic material, coming from bound diethylether and/or its derivatives, is released starting from about 110 °C which is indicated by a rise of the MS intensity at $m/z = 29$ (C_2H_5^+). The release is almost completed at the end of the first decomposition step, irrespective of whether the decomposition temperature is shifted towards higher temperatures due to the variation of the heating rate, or not. This indicates that the organic material is tightly bound and can—at these temperatures—be only released when the alanate is decomposed into MgH_2 , Al and H_2 .

3.2.3. Thermodynamic properties

We have been trying to determine equilibrium pressures of pure $\text{Mg}(\text{AlH}_4)_2$ by providing excess material in a small reactor for the desorption and measuring the hydrogen pressure, while the reactor has been submersed in an oil bath at a constant temperature. The temperatures have been varied in a range between 75 and 95 °C which coincides with the working temperature of a PEM fuel cell. The kinetics of the decomposition of the uncatalysed compound is very slow at these temperatures and every measurement takes several days to weeks. This might be a reason for the relatively large scatter of data we have found as even small leakages may cause relatively large errors in the measurement. The measured pressures have been in the range between 88 and 130 bar which is characteristic for a low temperature hydride. To rehydrogenate the material, higher pressures would have to be applied at this temperature level in order to provide a driving force for the back-formation of the alanate. It is intended to determine the reaction enthalpy also by other methods, such as HP-DSC.

4. Conclusion

The reversible weight content of hydrogen has to be increased and the thermodynamic and kinetic properties of aluminium hydrides have to be optimised before they can be regarded as suitable materials for hydrogen storage in combination with PEM fuel cells in mobile and automotive applications.

A large step has been made in improving the hydrogen exchange kinetics by a tailored catalyst which is a Ti colloid consisting of two-shell Ti clusters stabilised by THF ligands ($\text{Ti}_{13}\cdot 6 \text{ THF}$). A storage material which was produced by ball-milling pure NaAlH_4 with 2 mol% of Ti clusters for 30 min could be rehydrogenated to 80% within only 7 min, which is close to the technical target of 5 min.

Such a material would, however, not fulfil the requirement of storing more than 6 wt.% of hydrogen. In search for suitable storage materials, we have synthesised nanocrystalline magnesium alanate, $\text{Mg}(\text{AlH}_4)_2$, a compound which contains a theoretical amount of 9.3 wt.% hydrogen and which has been hardly investigated so far. The synthesis of gram amounts of the material is possible by a metathesis reaction of NaAlH_4 and MgCl_2 , followed by a purification procedure and thermal treatment in vacuum. According to theoretical (DFT) calculations and XRD, IR and Raman data the magnesium alanate exhibits a CdI_2 -like sheet structure with the Cd atoms replaced by MgH_6 octahedra and the I atoms replaced by AlH_4 tetrahedra. The spatial position of the H atoms still has to be verified experimentally.

In vacuum, the alanate decomposes at about 160 °C while three quarters of the bound hydrogen is released. The last quarter gets released at temperatures around 300 °C which is too high for a PEM fuel cell application. First measurements for determining equilibrium pressures indicate that $\text{Mg}(\text{AlH}_4)_2$ is a typical low temperature hydride. Reloading the decomposed material at the working temperatures

of a PEM fuel cell will require hydrogen pressures above 100 bar.

Acknowledgements

The authors would like to thank Petra Scheer and Lucia Fernandez for their assistance with the syntheses and the TGA–MS measurements. We are also grateful for beam-time allotment by ANKA and experimental assistance by the ANKA-ISS staff.

References

- [1] FY 2002 Progress Report for Hydrogen, Fuel Cells, and Infrastructure Technologies Program, US Department of Energy, November 2002 (<http://www.eere.energy.gov/hydrogenandfuelcells/pdfs/33098.toc.pdf>).
- [2] J. Töpler, O. Bernauer, H. Buchner, H. Säufferer, J. Less-Common Met. 89 (1983) 519–526.
- [3] J.A. Dilts, E.C. Ashby, Inorg. Chem. 11 (6) (1972) 1230.
- [4] B. Bogdanovic, M. Schwickardi, J. Alloys Compd. 253–254 (1997) 1–9.
- [5] K.J. Gross, G.J. Thomas, C.M. Jensen, J. Alloys Compd. 330–332 (2002) 683–690.
- [6] B. Bogdanovic, M. Felderhoff, M. Germann, M. Hartel, A. Pommerin, F. Schueth, C. Weidenthaler, B. Zibrowius, J. Alloys Compd. 350 (2003) 246–255.
- [7] M. Fichtner, O. Fuhr, O. Kircher, J. Rothe, Nanotechnology 14 (2003) 778–785.
- [8] L. Zaluski, A. Zaluska, J.O. Ström-Olsen, J. Alloys Compd. 290 (1999) 71–78.
- [9] E. Wiberg, R. Bauer, Z. Naturforschung 5b (1950) 397.
- [10] M. Fichtner, O. Fuhr, J. Alloys Compd. 345 (2002) 286–296.
- [11] R. Franke, J. Rothe, J. Pollmann, J. Hormes, H. Boennemann, W. Brijoux, Th. Hindenburg, J. Am. Chem. Soc. 118 (1996) 12090–12097.
- [12] P.S. Rudman, J. Less-Common Met. 89 (1983) 93–110.
- [13] M. Fichtner, J. Engel, O. Fuhr, A. Gloess, O. Rubner, R. Ahlrichs, Inorg. Chem. 42 (2003) 7060–7066.
- [14] M. Fichtner, O. Fuhr, O. Kircher, J. Alloys Compd. 356–357 (2003) 418–422.